

Density Functional Theory Study of the Interaction of Hydrogen with Li_6C_{60}

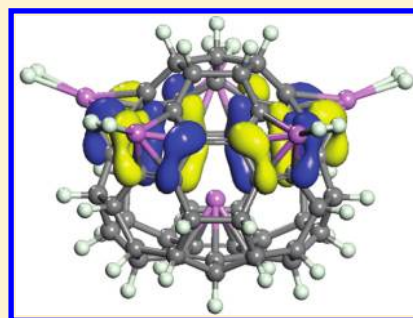
Qian Wang^{†,‡} and Puru Jena^{*,‡}

[†]Center for Applied Physics and Technology, College of Engineering, Peking University, Beijing 100871, China

[‡]Physics Department, Virginia Commonwealth University, Richmond, Virginia 23284, United States

ABSTRACT: Hydrogen storage properties of Li-coated C_{60} fullerene have been studied using density functional theory within the local density as well as generalized gradient approximation. Hydrogen atoms are found to bind to Li_6C_{60} in two distinct forms, with the first set attaching to C atoms, not linked to Li, in atomic form. Once all such C atoms are saturated with hydrogen, the second set of hydrogen atoms bind quasi-molecularly to the Li atoms, five of which remain in the exohedral and the sixth in the endohedral position. The corresponding hydrogen gravimetric density in $\text{Li}_6\text{C}_{60}\text{H}_{40}$ is 5 wt %. Desorption of hydrogen takes place in succession, the ones bound quasi-molecularly desorbing at a temperature lower than the ones bound atomically. The results are compared with the recent experiment on hydrogen adsorption in Li_6C_{60} .

SECTION: Energy Conversion and Storage; Energy and Charge Transport



Ideal hydrogen storage materials for mobile applications require the host material to be light and to operate at near-ambient thermodynamic conditions.^{1,2} For the latter requirement, hydrogen binding should be intermediate between physisorption and chemisorption. Unfortunately, lightweight materials such as Li and C bind hydrogen strongly. For example, in LiH, hydrogen desorbs at 670 °C,³ while in hydrogenated C_{60} fullerenes, C_{60}H_x (often referred to as fullerenes or hydrofullerenes), hydrogen desorbs at temperatures above 500 °C.^{4–9} In addition, the fullerenes release hydrocarbons during hydrogen desorption, thus making fullerenes unsuitable for reversible hydrogen storage.^{5,7,10,11} It was suggested¹² that one can avoid this problem by doping C_{60} with Li. Because C_{60} has a large electron affinity, charge transfer from Li to the C_{60} cage makes Li positively charged, and the electric field produced by such point charges can bind hydrogen through the polarization mechanism.^{13,14} In such a case, H_2 molecules are polarized and bind to Li in quasi-molecular form^{13,14} with a binding energy lying between physisorption and chemisorption. This makes it possible for hydrogen to desorb at near-ambient conditions. It was predicted that $\text{Li}_{12}\text{C}_{60}$ can reversibly store as much as 13 wt % hydrogen in quasi-molecular form.¹²

Recently Teprovich et al.¹⁵ have carried out an experiment using solvent-assisted mixing in which the mole ratio of LiH/ C_{60} was varied from 120:1 to 2:1. The authors found that Li_xC_{60} was capable of storing hydrogen reversibly through chemisorption at elevated temperatures and pressures. In particular, Li_6C_{60} with a mole ratio of 6:1 can reversibly desorb up to 5 wt % H_2 with an onset temperature of ~270 °C. In addition, the fullerene cage remained mostly intact and was only slightly modified during the desorption/adsorption cycle. Furthermore, no release of hydrocarbons was noticed. These

exciting results, however, leave some fundamental questions unanswered. (1) For example, where do Li atoms reside in C_{60} ? Do they occupy an exohedral or endohedral position? Do they cluster or remain isolated? (2) As Li doped C_{60} is hydrogenated, where do the hydrogen atoms reside? Do they bind to Li or C atoms and in what form? (3) What is the maximum number of H atoms that can bind to the Li_6C_{60} surface and does their binding energy depend upon the amount of hydrogen adsorbed? (4) Why does the Li_6C_{60} cage not break up and release hydrocarbons while the C_{60} fullerene does during dehydrogenation? (5) Why does hydrogen desorb at a much lower temperature in hydrogenated Li_6C_{60} than in fullerenes? In this Letter, we provide answers to some of these questions by carrying out detailed density functional theory based calculations. In the following, we give a brief description of our theoretical procedure, which is followed by a discussion of our results and a summary of our conclusions.

Site preference of Li and H atoms on C_{60} , the total energies of Li-decorated C_{60} with and without hydrogen loading, and the electronic structure of $\text{Li}_6\text{C}_{60}\text{H}_x$ were calculated using density functional theory and the Perdew–Burke–Ernzerhof (PBE)¹⁶ form for the generalized gradient-corrected (GGA) exchange–correlation functional. We used a plane wave basis set and the projector augmented wave method as implemented in the Vienna ab initio Simulation Package (VASP).¹⁷ The supercell approach was used where clusters were placed at the center of a $24 \times 24 \times 24 \text{ \AA}^3$ cubic cell. Due to the large supercell, the Brillouin zone integration was performed only at the Γ point. The energy cutoff was set at 400 eV. In all calculations, self-

Received: February 17, 2012

Accepted: April 9, 2012

Published: April 9, 2012

consistency was achieved with a tolerance in the total energy of at least 0.01 meV. Hellman–Feynman force components on each ion in the supercells were converged to 1 meV/Å. The structures were optimized without any symmetry constraint. In the case of hydrogen molecules binding weakly to the Li metal ions, calculations were repeated using local density approximation (LDA).¹⁸ This is because DFT does not treat dispersive forces properly and GGA is known to cause underbinding. On the other hand, LDA leads to overbinding and somehow compensates for the lack of dispersive forces in DFT. Test calculations have shown that binding energies in weakly coupled systems computed using LDA are in better agreement with those from experiment as well with those based on second-order Moller–Plesset perturbation theory (MP2)¹⁹ and the coupled cluster method with singles and doubles and noniterative inclusion of triples [CCSD(T)].²⁰ We have also performed IR stability calculations to ensure that the geometries presented in this Letter are dynamically stable and contain no imaginary frequencies.

Site Preference of Li As a Function of Li Concentration. We first discuss the geometry of Li_xC_{60} ($x = 1, 6$). To determine the preferred site of Li on C_{60} , we first calculated the total energies of LiC_{60} by placing the Li atom on the five-fold and six-fold hollow sites. The preferred site is one where Li binds to the five-fold site, while the one bound to the six-fold site is 60 meV higher in energy. This is in agreement with earlier calculations.¹²

The energy barrier when the Li atom moves from the pentagon to the hexagon site across a C–C bridge was calculated to be 0.35 eV by using the nudged elastic band (NEB) method implemented in VASP code. This barrier is larger than the 0.2 eV barrier in the (5,5) carbon nanotube²¹ when a Li atom moves across a C–C bridge from one hexagon to another along the nonaxial direction. Although C_{60} and the (5,5) carbon nanotube have very similar diameters, the pentagon to hexagon migration in C_{60} results in a larger energy barrier. Because this is much larger than the thermal energy corresponding to the room temperature, Li migration is unlikely under ambient thermodynamic conditions.

There are many possibilities for the geometry of Li_6C_{60} . Here, Li atoms may occupy near-neighbor sites, remain isolated from each other, or form either endohedral or exohedral complexes. In Figure 1, we provide the optimized geometry of four low-lying isomers of Li_6C_{60} with Li atoms having the freedom to occupy an exohedral or endohedral position as well as forming isolated or clustered configurations. The configuration with Li atoms bound to exohedral sites and occupying near-neighbor positions has the lowest energy, but the other geometries are energetically nearly degenerate. This is because there is virtually no interaction between the Li atoms because the Li–Li binding energy (1.10 eV) is much smaller than the Li–C binding energy (2.83 eV). In addition, the binding energy per Li atom in Li_xC_{60} , defined as

$$E_b(\text{Li}) = -[E(\text{Li}_x\text{C}_{60}) - E(\text{C}_{60}) - xE(\text{Li})]/x \quad (1)$$

is 1.53 eV for $x = 1$ and 1.76 eV for $x = 6$. The small difference in $E_b(\text{Li})$ suggests that Li atoms may randomly occupy five-fold sites in C_{60} . IR stability calculations confirmed the dynamical stability of the geometries with no imaginary frequencies. In Figure 2, we plot the highest occupied molecular orbital (HOMO) and the lowest unoccupied molecular orbital (LUMO) corresponding to the lowest-energy structure in Figure 1(a₁). We find that the C atoms in the two adjoining

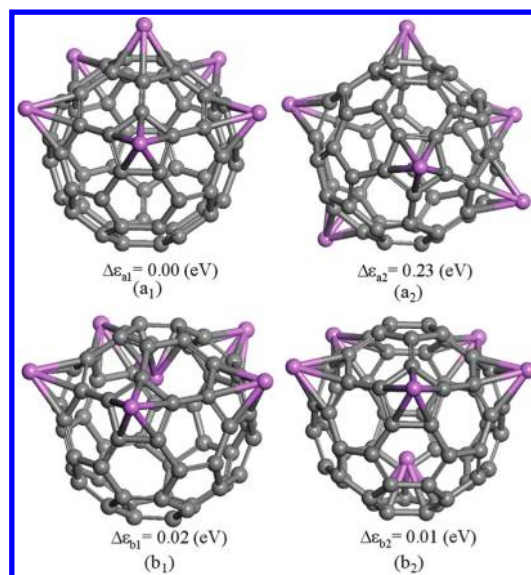


Figure 1. Geometries of the ground-state (a₁) and low-lying isomers (a₂), (b₁), and (b₂) of Li_6C_{60} clusters. Relative energies $\Delta\epsilon$ of each cluster with respect to the ground state are also given. The symmetries of (a₁), (b₁), and (a₂) structures are C_{5v} , while that of (b₂) is C_2 .

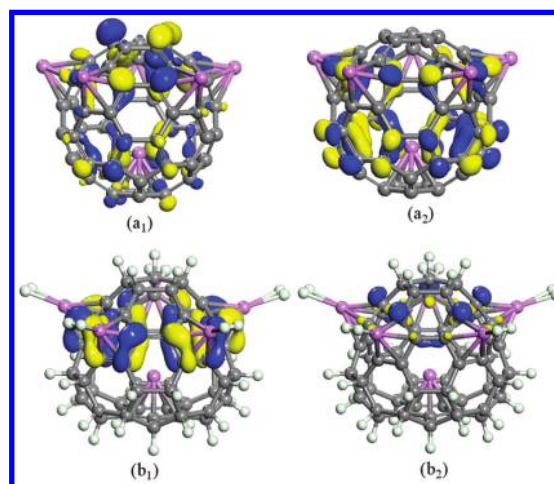


Figure 2. (a₁) HOMO and (a₂) LUMO of the Li_6C_{60} cluster with C_{5v} symmetry; (b₁) HOMO and (b₂) LUMO of the lowest-energy configuration of the Li_6C_{60} -40H cluster.

pentagons along the C_{5v} axis contribute more to the HOMO but not to the LUMO, as shown in Figure 2(a₁) and (a₂), respectively.

Site Preference of H As a Function of Li Concentration ($\text{Li}_x\text{C}_{60}\text{H}_y$). Using total energy calculations, we first determine the preferred site of one H atom in LiC_{60} by placing it atop the Li site. Next, we considered H atop the C atom nearest to the Li atom as well as the C site farthest from the Li atom. Again, the geometries are fully relaxed for each configuration. The resulting optimized geometries and relative energies measured with respect to the lowest-energy configuration are given in Figure 3. We note that the clearly preferred configuration for the H atom is where it attaches to the on-top C site that is nearest to the Li atom (Figure 4b). We define the binding energy of hydrogen as

$$E_b(\text{H}) = -[E(\text{LiC}_{60}\text{H}) - E(\text{LiC}_{60}) - E(\text{H})] \quad (2)$$

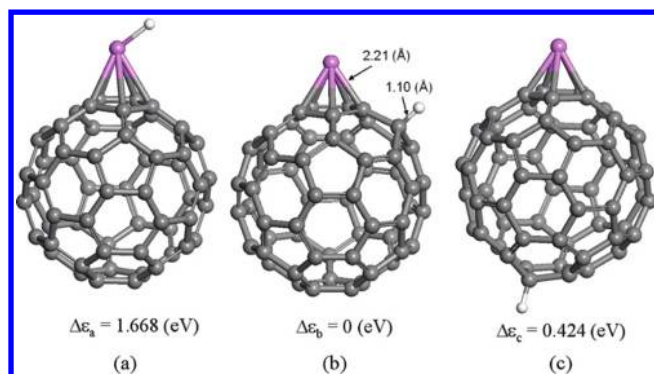


Figure 3. Geometries of the ground-state and low-lying isomers of the $\text{LiC}_{60}\text{-H}$ cluster. Interatomic distances and relative energies $\Delta\epsilon$ with respect to the ground state are also given.

This binding energy is 2.76 eV. This needs to be compared with the 3.58 eV binding energy of H to C in a CH dimer and the 2.34 eV binding energy of H to Li in a LiH dimer. This comparison establishes why H prefers to bind to C rather than to Li. To understand why H prefers to bind to a C atom that is nearest to the Li atom rather than to the one farthest removed, we note that H prefers to remain as a H^- ion. The charge transfer from Li to C_{60} puts extra electrons in the vicinity of the Li atom, enabling the C atoms nearest to C_{60} to donate electrons to H more easily.

We next consider the geometry of Li_6C_{60} decorated with 40 H atoms as this corresponds to 5 wt % hydrogen seen experimentally to desorb around 270 °C. The questions that need to be answered are as follows: (1) Where do these H atoms reside? (2) Does the location of the Li atoms on C_{60} change as more hydrogen atoms are adsorbed? (3) What is the average binding energy of H per atom in $\text{Li}_6\text{C}_{60}\text{H}_x$ and how does it compare to that in C_{60}H_x ? (4) Does the C_{60} cage remain unaffected as Li and H atoms are loaded? To answer these questions, six configurations were considered (see Figure 4). We first introduced H atoms on top of Li and C atoms in such a way that the 40 H atoms were distributed over the entire C_{60}

surface with H atoms binding to C or Li atoms [Figure 4(a₁)]. Second, we allowed the H atoms to cluster over the C_{60} surface [Figure 4(a₂)]. In the third configuration [Figure 4(a₃)], some of the H atoms were bound to Li atoms in quasi-molecular form, while others were bound to C atoms chemically. In these three configurations, the Li atoms were kept on exohedral sites. The calculations were repeated by allowing Li atoms to occupy both exohedral and endohedral positions. Three of the low-lying isomers, optimized without any symmetry constraint, are shown in Figure 4(b₁), (b₂), and (b₃). The relative energies measured with respect to the lowest-energy structure are given in Figure 4. Thermodynamically, the most stable structure [Figure 4(b₂)] is the one where five Li atoms remain on the outside, with each binding to one H_2 molecule in quasi-molecular form. The sixth Li atom becomes endohedral and does not bind to any H atom. The other 30 H atoms bind to 30 C atoms not coordinated with Li. The degeneracy between the Li_6C_{60} structures with five Li atoms on the outside and one Li atom on the inside versus that with all six Li atoms on the outside (see Figure 1) is lifted once H atoms are adsorbed. Note that the structure where six Li atoms are on the outside binding to five H_2 molecules [Figure 4(a₃)] is 2.53 eV higher in energy than the ground-state structure.

The ground-state structure in Figure 4(b₂) is interesting. Here, the C atoms linked to Li do not bind H. Because for each Li atom there are five such C atoms, a total of 30 C atoms in C_{60} cannot bind hydrogen. That leaves only 30 C atoms, each of which binds to one H atom. Because Li atoms are positively charged, they bind hydrogen in quasi-molecular fashion due to the charge polarization mechanism discussed earlier.^{13,14} Thus, five Li atoms bind five H_2 molecules, and the geometry in Figure 4(b₂) completely accounts for all of the H atoms attached in $\text{Li}_6\text{C}_{60}\text{H}_{40}$. We also note that the structure of the C_{60} cage gets distorted as Li and H atoms are bound.

In order to better understand the lowest-energy structure of $\text{Li}_6\text{C}_{60}\text{H}_{40}$ as shown in Figure 4(b₂), where one Li atom is inside of the cage, we calculated the energy barrier that needs to be overcome by Li for insertion into the cage. One possible scenario is that at high temperature, one Li atom may diffuse

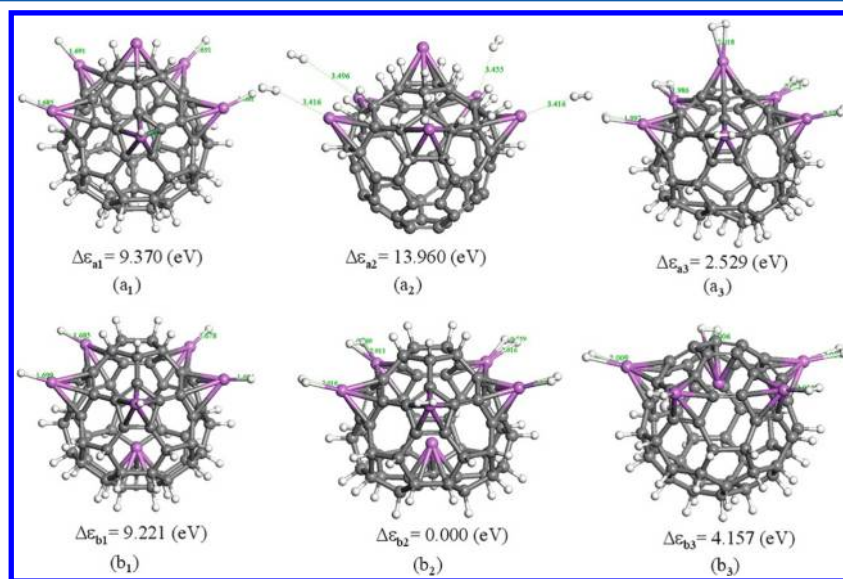


Figure 4. Geometries of the ground state (b₂) and the other five low-lying isomers of the $\text{Li}_6\text{C}_{60}\text{H}_{40}$ cluster. Relative energies $\Delta\epsilon$ with respect to the ground state of each cluster are given.

from one pentagon to the nearest hexagon from which it can enter into the cage. We, therefore, calculated this energy barrier, which was found to be 6.95 eV. While this is very large, we note that it is smaller than the penetration energy barrier of 7.40 eV on a graphene sheet.²² This can be understood with the following two factors: First, in C_{60} , the longer C–C bond between a hexagon and a pentagon is 1.458 Å, and the shorter C–C bond length between the two hexagons is 1.40 Å.²³ The average C–C bond length in a hexagon is 1.429 Å, which is larger than that (1.40 Å) in the graphene sheet. Second, due to the curvature of the C_{60} surface, the p_z orbitals are orientated more outwardly, which would further reduce the energy barrier when the Li atom enters the cage. It is likely that under experimental conditions,¹⁵ all of the Li atoms may reside on the exohedral positions. In that case, the sixth Li atom can also bind to one H_2 molecule, thus increasing the number of hydrogen atoms from 40 to 42. Note that the exact number of H atoms attached to Li_6C_{60} was not determined in the above experiment, and the authors estimated it to be around 40.

Binding Energy of Hydrogen to C_{60} versus Li_xC_{60} . As mentioned earlier, the binding energy of a H atom to C_{60} decorated with a single Li atom is 2.76 eV. In order to see how this binding energy changes with respect to multiple hydrogen decoration, we first consider the average binding energy of H in the $Li_6C_{60}H_{30}$ cluster. Here, H atoms are bound to the 30 C atoms that are not linked to Li. The average H binding energy is defined as

$$\langle E_b(H) \rangle = -[E(Li_6C_{60}H_{30}) - E(Li_6C_{60}) - 30E(H)]/30$$

We find $\langle E_b(H) \rangle$ to be 2.64 eV. Because this is rather close to the binding energy of 2.76 eV in $LiC_{60}H$, one can conclude that the binding energy of H is not very sensitive to the number of Li atoms that decorate C_{60} . To examine how these binding energies compare with that in pristine C_{60} , we have calculated the optimized structures of $C_{60}H_{30}$ and $C_{60}H_{60}$ clusters. While there is no ambiguity in the structure of $C_{60}H_{60}$ as there is one H atom for every C atom, there are numerous choices for the possible structure of $C_{60}H_{30}$. We considered an initial geometry for $C_{60}H_{30}$ by removing the six Li atoms and five quasi-molecularly bound H_2 's from Figure 4(b₂). The structure was then reoptimized. The calculated average binding energies of the H atom in the $C_{60}H_{30}$ and $C_{60}H_{60}$ clusters were 2.54 and 2.44 eV, respectively. These energies are slightly smaller than those in $Li_6C_{60}H_{30}$, namely, 2.64 eV. In other words, hydrogen binds more strongly to Li-coated C_{60} than to pristine C_{60} . The question then remains, Why does hydrogen desorb from $Li_6C_{60}H_y$ at a lower temperature than that from $C_{60}H_y$? Thermodynamically this should not be the case because H is bound to C in $Li_6C_{60}H_{30}$ at least as strongly as that in Li_6C_{60} .

We note that in $Li_6C_{60}H_{40}$, 10 H atoms are bound quasi-molecularly to the Li atoms. The binding energy of these H atoms is clearly less than that for the ones bound in atomic form. To see what this binding energy is, we calculated the energy needed to desorb only the H atoms bound quasi-molecularly using the equation

$$\langle E_b(H_2) \rangle = -[E(Li_6C_{60}5H_2) - E(Li_6C_{60}) - 5E(H_2)]/5$$

This yields a binding energy of 0.14 eV. The corresponding energy when C_{60} contains only one Li atom is 0.17 eV. The substantial reduction in binding energy between H atoms bound quasi-molecularly versus those bound chemically to the C atoms is due to the different mechanisms operative in the bonding scheme. In the former, the bonding is due to a

polarization mechanism that is not chemical in nature and hence is weak.^{13,14} We should caution the reader that density functional theory with GGA functional does not include dispersive forces and hence always leads to underbinding. Because DFT within LDA leads to overbinding, it is expected that calculations at the DFT/LDA level of theory may compensate for this omission and may yield a more realistic binding energy when dealing with weak polarization forces. We, therefore, repeated the above calculations using DFT/LDA with the Vosko–Wills–Nussair (VWN) formula.²⁴ The resulting $\langle E_b(H) \rangle$ was found to be 0.28 eV, which is significantly larger than that obtained using the DFT/GGA formalism.

Leaving quantitative comparison aside, we can confidently conclude that there are two types of H atoms bound in Li_6C_{60} with very different binding energies. The ones bound more weakly, namely, the quasi-molecular species, will desorb at a lower temperature, while those bound more strongly to the C atom will require elevated temperatures. We should point out that if only the quasi-molecular hydrogen atoms are seen experimentally to reversibly adsorb on Li_6C_{60} , the gravimetric density should be 1.25 wt % and not 5 wt % as observed. To reconcile this apparent discrepancy, we note that as many as five H_2 molecules can be bound¹² to a Li atom in free $Li_{12}C_{60}$. However, when the $Li_{12}C_{60}$ clusters interact as they would in a solid-state environment, the Li atoms bonding the two C_{60} fullerenes cannot bind hydrogen, thus reducing their total hydrogen uptake. Gravimetric density of 5 wt % hydrogen storage in bulk Li_6C_{60} can be achieved if each of the five exohedral Li atoms can bind to four H_2 molecules.

Our results also explain why dehydrogenation of fullerenes leads to breaking up of the cage structure and emission of hydrocarbons while similar effects are not present in Li_6C_{60} . We recall that the binding energy of atomic hydrogen in Li_6C_{60} is larger than that in C_{60} . Thus, the temperature required to break up Li_6C_{60} will be higher than that of C_{60} . This may be a likely cause for the enhanced stability of the Li_6C_{60} cage during repeated adsorption/desorption cycles. Hydrogen atoms that are seen to desorb from Li_6C_{60} at lower temperatures are those that are bound more weakly than the ones bound in atomic form.

In summary, we have carried out a systematic and comprehensive study to determine the site preference of Li on C_{60} , the sites that hydrogen atoms occupy as a function of Li concentration, the nature of hydrogen bonding as a function of hydrogen concentration, and their corresponding binding energy. While Li atoms prefer to occupy exohedral sites in C_{60} , the structure with one Li atom in the endohedral position is nearly degenerate. However, this degeneracy is lifted once hydrogen atoms are present. For example, in the $Li_6C_{60}H_{40}$ structure, one of the Li atoms prefers to remain in the endohedral position. We find that hydrogen atoms bind more strongly to C atoms in Li-coated C_{60} compared to that in pure C_{60} . There are two types of hydrogen bonding in Li_6C_{60} ; the first set of hydrogen binds to C in atomic form, and subsequent H atoms bind to Li in quasi-molecular form. Forty H atoms can be adsorbed on Li_6C_{60} , where 30 of them are bound to C atoms in atomic form and 10 of them to Li in quasi-molecular form. Because the former binding is much stronger than the latter, this permits hydrogen atoms to desorb in successive steps. We should caution the reader that our calculations did not take into account van der Waal and zero-point energy corrections. Grimme²⁵ has pointed out that the GGA exchange–correlation usually underestimates the binding energy by ~ 0.08 eV/ H_2 .

Zero-point energy correction, on the other hand, reduces the binding energy by about 20%. Because these two omissions compensate for each other, we believe that our conclusions are qualitatively correct. We also note that while these studies are performed on an isolated C_{60} cluster, experiments were carried out in bulk samples where interaction between C_{60} clusters may also be important. However, prior studies¹² showed that the structure of the Li-coated C_{60} remained intact during such interactions, and three H_2 molecules could still be bound to each Li atom. We are currently carrying out studies of hydrogen storage properties of Li_6C_{60} cluster-assembled materials to get a quantitative understanding of hydrogen sorption.

AUTHOR INFORMATION

Corresponding Author

*E-mail: pjena@vcu.edu

Notes

The authors declare no competing financial interest.

ACKNOWLEDGMENTS

This work was supported in part by grants from the US Department of Energy and the National Natural Science Foundation of China (Grant No. NSFC-11174014). This research used resources of the National Energy Research Scientific Computing Center, which is supported by the Office of Science of the U.S. Department of Energy under Contract No. DE-AC02-05SCH11231.

REFERENCES

- (1) Jena, P. Materials for Hydrogen Storage: Past, Present, and Future. *J. Phys. Chem. Lett.* **2011**, *2*, 206–211.
- (2) U.S. DOE; USCAR; Shell; BP; Conoco Phillips; Chevron; Exxon Mobil; The FreedomCAR and Fuel Partnership *Multi-Year Research, Development and Demonstration Plan*. <http://www1.eere.energy.gov/hydrogenandfuelcells/mypp/pdfs/storage.pdf> (2009).
- (3) Kawano, H.; Tanaka, A.; Sugimoto, S.; Iseki, T.; Zhu, Y.; Wada, M.; Sasao, M. Selection of the Powdery Metal Hydride Best for Producing H^- by Thermal Desorption. *Rev. Sci. Instrum.* **2000**, *71*, 853.
- (4) Bausch, J. W.; Prakash, G. K. S.; Olah, G. A.; Tse, D. S.; Lorents, D. C.; Bae, Y. K.; Malhotra, R. J. Diamagnetic Polyanions of the C_{60} and C_{70} Fullerenes: Preparation, ^{13}C and 7Li NMR Spectroscopic Observation, And Alkylation with Methyl Iodide to Polymethylated Fullerenes. *J. Am. Chem. Soc.* **1991**, *113*, 3205–3206.
- (5) Talyzin, A. V.; Shulga, Y. M.; Jacob, A. Comparative Study of Hydrofullerides $C_{60}H_x$ Synthesized by Direct and Catalytic Hydrogenation. *Appl. Phys. A: Mater. Sci. Process.* **2004**, *78*, 1005–1010.
- (6) Talyzin, A. V.; Tsybin, Y. O.; Schaub, T. M.; Mauron, P.; Shulga, Y. M.; Zuttel, A.; Sundqvist, B.; Marshall, A. G. Composition of Hydrofullerene Mixtures Produced by C_{60} Reaction with Hydrogen Gas Revealed by High-Resolution Mass Spectrometry. *J. Phys. Chem. B* **2005**, *109*, 12742–12747.
- (7) Brosha, E. L.; Davey, J.; Garzon, F. H.; Gottesfeld, S. Irreversible Hydrogenation of Solid C_{60} with and without Catalytic Metals. *J. Mater. Res.* **1999**, *14*, 2138–2146.
- (8) Luzan, S. M.; Tsybin, Y. O.; Talyzin, A. V. Reaction of C_{60} with Hydrogen Gas: In Situ Monitoring and Pathways. *J. Phys. Chem. C* **2011**, *115*, 11484–11492.
- (9) Talyzin, A. V.; Sundqvist, B.; Shulga, Y. M.; Peera, A. A.; Imus, P.; Billups, W. E. Gentle Fragmentation of C_{60} by Strong Hydrogenation: A Route to Synthesizing New Materials. *Chem. Phys. Lett.* **2004**, *400*, 112–116.
- (10) Osaki, T.; Tanakab, T.; Tai, Y. Hydrogenation of C_{60} on Alumina-Supported Nickel and Thermal Properties of $C_{60}H_{36}$. *Phys. Chem. Chem. Phys.* **1999**, *1*, 2361–2366.
- (11) Wang, N.; Zhang, J. Preparation and Decomposition of $C_{60}H_{36}$. *J. Phys. Chem. A* **2006**, *110*, 6276–6278.
- (12) Sun, Q.; Jena, P.; Wang, Q.; Marquez, M. First-Principles Study of Hydrogen Storage on $Li_{12}C_{60}$. *J. Am. Chem. Soc.* **2006**, *128*, 9741–9745.
- (13) Niu, J.; Rao, B. K.; Jena, P. Binding of Hydrogen Molecules by a Transition-Metal Ion. *Phys. Rev. Lett.* **1992**, *68*, 2277–2280.
- (14) Rao, B. K.; Jena, P. Hydrogen Uptake by an Alkali Metal Ion. *Euro. Phys. Lett.* **1992**, *20*, 307.
- (15) Teprovich, J. A., Jr.; Wellons, M. S.; Lascola, R.; Hwang, S.-J.; Ward, P. A.; Compton, R. N.; Zidan, R. Synthesis and Characterization of a Lithium-Doped Fullerene ($Li_x-C_{60}-H_y$) for Reversible Hydrogen Storage. *Nano Lett.* **2012**, *12*, 582–589.
- (16) Perdew, J. P.; Burke, K.; Ernzerhof, M. Generalized Gradient Approximation Made Simple. *Phys. Rev. Lett.* **1996**, *77*, 3865–3868.
- (17) Kresse, G.; Furthmüller, J. Efficient Iterative Schemes for Ab Initio Total-Energy Calculations Using a Plane-Wave Basis Set. *Phys. Rev. B* **1996**, *54*, 11169–11186.
- (18) Ceperley, D. M.; Alder, B. J. Ground State of the Electron Gas by a Stochastic Method. *Phys. Rev. Lett.* **1980**, *45*, 566–569.
- (19) Møller, C.; Plesset, M. S. Note on an Approximation Treatment for Many-Electron Systems. *Phys. Rev.* **1934**, *46*, 618–622.
- (20) Raghavachari, K.; Trucks, G. W.; Pople, J. A.; Head-Gordon, M. A Fifth-Order Perturbation Comparison of Electron Correlation Theories. *Chem. Phys. Lett.* **1989**, *157*, 479–483.
- (21) Zhao, M.; Xia, Y.; Mei, L. Diffusion and Condensation of Lithium Atoms in Single-Walled Carbon Nanotubes. *Phys. Rev. B* **2005**, *71*, 165413.
- (22) Khantha, M.; Cordero, N. A.; Alonso, J. A.; Cawkwell, M.; Girifalco, L. A. Interaction and Concerted Diffusion of Lithium in a (5,5) Carbon Nanotube. *Phys. Rev. B* **2008**, *78*, 115430.
- (23) Hedberg, K.; Hedberg, L.; Bethune, D. S.; Brown, C. A.; Dorn, H. C.; Johnson, R. D.; Vries, M. D. Bond Lengths in Free Molecules of Buckminsterfullerene, C_{60} , from Gas-Phase Electron Diffraction. *Science* **1991**, *254*, 410–412.
- (24) Vosko, S. H.; Wilk, L.; Nusair, M. Accurate Spin-Dependent Electron Liquid Correlation Energies for Local Spin Density Calculations: A Critical Analysis. *Can. J. Phys.* **1980**, *58*, 1200–1211.
- (25) Grimme, S. Accurate Description of van der Waals Complexes by Density Functional Theory Including Empirical Corrections. *J. Comput. Chem.* **2004**, *25*, 1463–1472.